Published in IET Generation, Transmission & Distribution
Received on 13th January 2011
Revised on 2nd September 2011
doi: 10.1049/iet-gtd.2011.0429

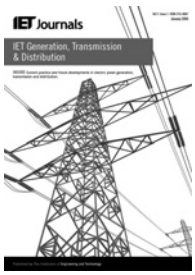

ISSN 1751-8687

New network sensitivity-based approach for real-time complex power flow calculation

W.-T. Huang K.-C. Yao

Department of Industrial Education and Technology, National Changhua University of Education, No. 2, Shida Road, Changhua 500, Taiwan
E-mail: vichuang@cc.ncue.edu.tw

Abstract: This study proposes a novel network sensitivity-based approach to solving complex power flow calculation problems in real time. A new sensitivity factor, named Jacobian-based distribution factor (JBDF), is used for the calculation of active and reactive power flow in transmission systems. It is derived from the Jacobian matrix of the base case Newton–Raphson power flow solution, and kept constant during real-time line flow calculation. Unlike well-known distribution factors, such as generation shift distribution factor (GSDF), generalised generation shift distribution factor (GGDF) and Z-bus distribution factor (ZBD), this approach reflects changes in complex injection power. Changes in load conditions from base case loads, with either conforming or non-conforming changes in complex power in each bus, can be used to rapidly compute active and reactive power flow without iterations. The proposed approach was tested on IEEE 14-Bus and 30-Bus systems. Numerical results demonstrate that the proposed approach is not only superior to previous distribution factors, but also compares favourably with the Newton–Raphson power flow method. It is well suited to real-time applications in steady-state security control and optimal dispatch.

1 Introduction

In AC power systems, power flow analysis is vitally important in the planning and operation stages. Particularly in the operation stage, power flow solutions including active and reactive power flows in transmission lines, together with bus voltage profiles, indicate the present system state. Reactive power plays an important role in power systems, in maintaining bus voltages within specified limits. As for prior contingencies, drops in voltage related to reactive power contributed to blackouts in the western USA in 1996 and France in 1978, and significant voltage swings because of reactive power in the mid-west and northeast USA in 2003. In addition, the major purpose of reactive power dispatch is to improve voltage profiles and minimise real power transmission loss, while satisfying unit and system constraints. In addition, active power balance is the dominant factor in maintaining the system in a stable state. Active power generation changes according to load demands and system losses. This involves the most important information with which operators grasp present active and reactive power flow in power system, representing the basis of real-time economic dispatch, security assessment and contingency analysis. Computation speed and the accuracy of solutions are key problems in ensuring that power systems are operating under secure conditions. Until now, the rapidity and accuracy of computation in power flow studies have been the goals of researchers of such system. However, full Newton power flow for real-time line flow calculation is computationally expensive. This study proposes a fast, reliable method, comprising the Newton–Raphson algorithm and Jacobian-based distribution factor (JBDF) for line flow calculation in real-time power system applications to speed up computation.

Conventionally, line flow has been calculated by executing an AC power flow program. The power flow program can be modelled by a set of non-linear simultaneous equations, approached by numerical iterative methods. Well-known approaches include the Gauss–Seidel [1], the Newton–Raphson [1] and the Fast Decoupled method [2]. Owing to the many iterations required to converge, the Gauss–Seidel method is not suitable for real-time applications. The Newton–Raphson approach can solve the problem with few iterations, but convergence is always a problem, because of its dependence on initial values. Executing the Gauss–Seidel program for several iterations to identify suitable initial values, and then performing the Newton–Raphson program is a feasible approach in some applications involving complex power systems. Stott and Alsac [2] proposed the fast decoupled method to overcome the computational burden of the power flow problem. Based on the concepts of DC power flow, this approach solves simultaneous power flow equations by $\boldsymbol{B}'$ and $\boldsymbol{B}''$ constant matrices, instead of the Jacobian matrix of the Newton method. Because there is no need for complex computation in the formation of the Jacobian matrix, it rapidly solves power flow equations; however, it still requires more iterations than the Newton method. In recent studies, specialised algorithms have been proposed to enhance robustness and efficiency to improve the problem of

convergence, [3–8]; however, these algorithms must still perform the iteration process during the solution procedure. If the number of iterations could be reduced or eliminated, the real-time application of these algorithms would be more reliable and feasible. Consequently, to improve computation speed and eliminate the need for iterations, various approaches involving network sensitivity factors have been proposed, the most well known of which are: generation shift distribution factor (GSDF) [1], generalised generation shift distribution factor (GGDF) [9], Z-bus distribution factor (ZBD) [10] and power transfer distribution factor (PTDF) [11, 12]. Based on the concept of DC power flow equations [1], GSDF factor expresses the active power line flows as incremental models of bus generation shifts. During economic dispatch and security computation, it is capable of rapidly responding to shifts in generation into the actual line flows from the base case solution. Despite its simplicity and wide application, it has problems in real-time applications in that total load demands are assumed to remain unchanged. Therefore it is only suitable for situations in which the total generating powers remains unchanged but shifts from some PV buses to other buses.

Ng [9] presented a novel approach to solve the real-time line flow calculation problem associated with the weakness of the GSDF factor, known as the GGDF sensitivity factor. It formulates active power flow as a function of bus generating power, rather than incremental models. According to these formulas, constrained active power flow models are easily constructed and rapidly calculated during iterations. The GGDF has been successfully applied in real-time applications of constrained economic dispatch [13] and optimal power flow [14] problems. Despite its features and performance, the GGDF remains problematic, because of its assumption of conforming load changes from the base case. In non-conforming load change cases, the GGDF loses much of its accuracy in line flow solutions [15]. This often restricts the practical application of GGDF.

The two above approaches are both based on DC power flow models. In such models, line flow reactance is only attended to, whereas line resistance is neglected. To overcome this shortcoming, a new sensitivity factor, termed ZBD, was proposed by Lin *et al.* [15]. Instead of using an $\boldsymbol{X}$ matrix, this approach formulates active power flow using the Z-Bus matrix. The ZBD is capable of representing any changes in load within the line flow, even if the changes are non-conforming. As demonstrated in [10], the accuracy of the ZBD line flow solution is much higher than that of the GSDF and GGDF approaches. The derivation and performance of PTDF are similar to the ZBD, and referring to recent research, sensitivity-based approaches have been widely proposed and applied in related studies into the control and operation of power systems. Fang *et al.* [16] developed a new sensitivity-based generation rescheduling method for the dynamic enhancement of security in power systems, and Ruiz and Sauer [17] used sensitivity to estimate post-contingency voltage and reactive power generation and flow. Parida *et al.* [18] proposed a value-based sensitivity approach for reactive power cost allocation; in addition Jupe and Taylor [19] presented power flow sensitivity factors for the online control of power output of distributed generation and Zhou and Bialek [20] developed voltage and loss sensitivity factors for generation curtailment. Teng and Lu [21] used a sensitivity factor calculation to determine better candidate locations for the placement of fault current limiters and Ayres *et al.* [22] proposed voltage sensitivity as a means to determine the maximum allowable penetration of distributed generation without violations in steady-state voltage. It can be concluded that few studies have used fast line flow calculation using a sensitivity-based approach. Nevertheless, the studies mentioned above have demonstrated theoretical feasibility and practical value in the application of power systems.

This paper proposes a new sensitivity factor termed the JBDF dealing with the problem using partial derivatives of the base case power flow Jacobian matrix. Unlike the four sensitivity factors above, which are only concerned with the active power changes, the JBDF reflects changes in bus active and reactive injection power within the reactive power flows. For any conforming or non-conforming changes in bus active and reactive power injection, reactive power flow can be easily and rapidly calculated using JBDF sensitivity factors without any iterations. The proposed approach was tested on IEEE 14-Bus and 30-Bus test systems. The theoretical basis, formulas and numerical results are described and discussed in detail in the following sections.

2 Derivation of JBDF

The derivation of the JBDF formulas is detailed in the following. Fig. 1 shows a schematic diagram of the transmission line m from bus p to bus q, in which active and reactive power flow can be expressed as a function of bus voltage magnitude and phase angle. It can be written as

$$P_m = G_m|V_p|^2 - G_m|V_p||V_q|\cos(\delta_p - \delta_q) - B_m|V_p||V_q|\sin(\delta_p - \delta_q) \quad (1)$$

$$Q_m = -B_m|V_p|^2 + B_m|V_p||V_q|\cos(\delta_p - \delta_q) - G_m|V_p||V_q|\sin(\delta_p - \delta_q) \quad (2)$$

where P_m and Q_m denote active and reactive power flow on arbitrary line m; $|V_p|$, $|V_q|$ and δ_p, δ_q denote the voltage magnitude and phase angles for bus p and q; G_m and B_m represent the conductance and acceptance of line m. In economic dispatch and optimal power flow applications, active and reactive powers are adjusted in each iteration. In conventional power flow algorithms, line flow is recomputed using the power flow program in each iteration to accommodate changes in bus power injection. This complicates computation, making it more time-consuming. Therefore to implement an efficient real-time dispatching law applicable for small variations of demand, the first-order sensitivity relationships was proposed in [23], and its development and application for determining corrective adjustments in active power flows by controlling the active power generation was also proposed in [24]. Based on the aspect mentioned in [23, 24], the concept and theory of JBDF is discussed roughly, and then the mathematical models of both the active and reactive sensitivity factors are derived.

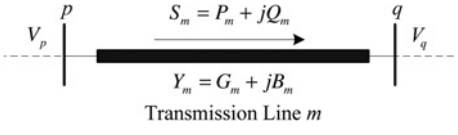

Fig. 1 *Schematic diagram of a transmission line segment*

doi: 10.1049/iet-gtd.2011.0429

2.1 Active power JBDF

In this subsection, the active power flow of line m can be modelled as the base case active power flow (P_m^0) plus incremental active power flow (ΔP_m), that is

$$P_m = P_m^0 + \Delta P_m \tag{3}$$

This is the concept of a sensitivity factor. Furthermore, the incremental active power flow of line m can be modelled as a function of the bus power injection according to the partial derivative of (1) with respect to variables P_i and Q_i, expressed as

$$\Delta P_m = \sum_{i=1}^{\mathrm{NB}} \frac{\partial P_m}{\partial P_i}\Delta P_i + \sum_{i=1}^{\mathrm{NB}} \frac{\partial P_m}{\partial Q_i}\Delta Q_i \tag{4}$$

In the above equation, the partial differential terms $\partial P_m/\partial P_i$ and $\partial P_m/\partial Q_i$ represent the sensitivity of bus i to line m, from bus p to bus q. Additionally, ΔP_i and ΔQ_i represent the increments of active and reactive power in bus i; NB denotes the bus number of the system. These terms can be replaced by $F_p(m, i)$, and $K_p(m, i)$, termed the active power JBDF. Consequently, (4) can be rewritten as

$$\Delta P_m = \sum_{i=1}^{\mathrm{NB}} F_p(m, i)\Delta P_i + \sum_{i=1}^{\mathrm{NB}} K_p(m, i)\Delta Q_i \tag{5}$$

Substituted from (4) for ΔP_m in (3)

$$P_m = P_m^0 + \sum_{i=1}^{\mathrm{NB}} F_p(m, i)\Delta P_i + \sum_{i=1}^{\mathrm{NB}} K_p(m, i)\Delta Q_i \tag{6}$$

In practical power systems, any changes in bus power injection cause variations in all bus voltage magnitudes and phase angles. Therefore the active power JBDF terms can be derived as follows

$$F_p(m, i) = \sum_{j=1}^{\mathrm{NB}} \frac{\partial |V_j|}{\partial P_i}\frac{\partial P_m}{\partial |V_j|} + \sum_{j=1}^{\mathrm{NB}} \frac{\partial \delta_j}{\partial P_i}\frac{\partial P_m}{\partial \delta_j}, \quad m = 1, 2, \ldots, \mathrm{NL} \tag{7}$$

and

$$K_p(m, i) = \sum_{j=1}^{\mathrm{NB}} \frac{\partial |V_j|}{\partial Q_i}\frac{\partial P_m}{\partial |V_j|} + \sum_{j=1}^{\mathrm{NB}} \frac{\partial \delta_j}{\partial Q_i}\frac{\partial P_m}{\partial \delta_j}, \quad m = 1, 2, \ldots, \mathrm{NL} \tag{8}$$

where NL denotes the number of lines in the system. In (7) and (8), the partial differential terms $\partial |V_j|/\partial |P_j|$, $\partial \delta/\partial P_i$, $\partial |V_j|/\partial Q_i$ and $\partial \delta_j/\partial Q_i$ can be calculated in the Jacobian matrix of the base case power flow solution. In the Newton–Raphson algorithm, iterative power flow equations can be expressed as

$$\begin{bmatrix} \Delta P \\ \Delta Q \end{bmatrix} = \begin{bmatrix} J_1 & J_2 \\ J_3 & J_4 \end{bmatrix} \begin{bmatrix} \Delta \delta \\ \Delta |V| \end{bmatrix} \tag{9}$$

Moreover, the inverse form of the above equations can be written as

$$\begin{bmatrix} \Delta \delta \\ \Delta |V| \end{bmatrix} = \begin{bmatrix} JB_1 & JB_2 \\ JB_3 & JB_4 \end{bmatrix} \begin{bmatrix} \Delta P \\ \Delta Q \end{bmatrix} \tag{10}$$

In which, JB_1 is the term of $\partial \delta/\partial P$; JB_2 is the term of $\partial \delta/\partial Q$; JB_3 is the term of $\partial |V|/\partial P$; JB_4 is the term of $\partial |V|/\partial Q$. In the base case power flow solution, these terms can be calculated using the Newton power flow program, kept constant during real-time computation when load levels deviate from base case loading conditions. Because line m is from bus p to bus q, active power flow P_m is only related to $|V_p|$, $|V_q|$, δ_p and δ_q. Therefore the summation of the differential terms in (7) and (8) can be reduced to

$$F_p(m, i) = \left(\frac{\partial |V_p|}{\partial P_i}\right)\frac{\partial P_m}{\partial |V_p|} + \left(\frac{\partial |V_1|}{\partial P_i}\right)\frac{\partial P_m}{\partial |V_q|} + \left(\frac{\partial \delta_p}{\partial P_i}\right)\frac{\partial P_m}{\partial \delta_p} + \left(\frac{\partial \delta_q}{\partial P_i}\right)\frac{\partial P_m}{\partial \delta_q} \tag{11}$$

$$K_p(m, i) = \left(\frac{\partial |V_p|}{\partial Q_i}\right)\frac{\partial P_m}{\partial |V_p|} + \left(\frac{\partial |V_q|}{\partial Q_i}\right)\frac{\partial P_m}{\partial |V_q|} + \left(\frac{\partial \delta_p}{\partial Q_i}\right)\frac{\partial P_m}{\partial \delta_p} + \left(\frac{\partial \delta_q}{\partial Q_i}\right)\frac{\partial P_m}{\partial \delta_q} \tag{12}$$

In (11) and (12), partial differential terms can be classified into two groups. In the first group, it is the relationships between bus voltage and bus power injection, where $\partial |V_p|/\partial P_i$, $\partial |V_q|/\partial P_i$, $\partial \delta_p/\partial P_i$ and $\partial \delta_q/\partial P_i$ are the elements of JB_3 and JB_1, respectively. And the partial differential terms of $\partial |V_q|/\partial Q_i$, $\partial |V_q|/\partial Q_i$, $\partial \delta_p/\partial Q_i$ and $\partial \delta_q/\partial Q_i$ are the elements of JB_4 and JB_2, respectively. In the section group, it is the relationships between active-power line flow and bus voltage. By differentiating (1), the partial differential terms of $\partial P_m/\partial |V_p|$, $\partial P_m/\partial |V_q|$, $\partial P_m/\partial \delta_p$ and $\partial P_m/\partial \delta_q$ can be expressed as (13)–(16)

$$\frac{\partial P_m}{\partial |V_p|} = 2|V_p^0|G_m - |V_q^0|G_m \cos(\delta_p^0 - \delta_q^0) - |V_q^0|B_m \sin(\delta_p^0 - \delta_q^0) \tag{13}$$

$$\frac{\partial P_m}{\partial |V_q|} = -|V_p^0|G_m \cos(\delta_p^0 - \delta_q^0) - |V_p^0|B_m \sin(\delta_p^0 - \delta_q^0) \tag{14}$$

$$\frac{\partial P_m}{\partial \delta_p} = |V_p^0||V_q^0|G_m \sin(\delta_p^0 - \delta_q^0) - |V_p^0||V_q^0|B_m \cos(\delta_p^0 - \delta_q^0) \tag{15}$$

and

$$\frac{\partial P_m}{\partial \delta_q} = -|V_p^0||V_q^0|G_m \sin(\delta_p^0 - \delta_q^0) + |V_p^0||V_q^0|B_m \cos(\delta_p^0 - \delta_q^0) \tag{16}$$

where $|V_p^0|$, $|V_q^0|$, δ_p^0 and δ_q^0 denote voltage magnitude and phase angle at bus p and bus q in base case loading conditions, respectively.

Using the above equations, the active power JBDF sensitivity factors can be calculated in base case loading conditions, and kept constant during real-time computations.

2.2 Reactive power JBDF

The derivation of reactive power JBDF is similar to active power JBDF, the reactive power flow of line m can be modelled as the base case reactive power flow (Q_m^0) plus incremental reactive power flow (ΔQ_m), that is

$$Q_m = Q_m^0 + \Delta Q_m \tag{17}$$

The incremental reactive power flow of line m can be modelled as the function of the bus power injection by the partial derivative of (2) with respect to variables P_i and Q_i, expressed as

$$\Delta Q_m = \sum_{i=1}^{\mathrm{NB}} \frac{\partial Q_m}{\partial P_i}\Delta P_i + \sum_{i=1}^{\mathrm{NB}} \frac{\partial Q_m}{\partial Q_i}\Delta Q_i \tag{18}$$

in which, the partial differential terms $\partial Q_m/\partial P_i$ and $\partial Q_m/\partial Q_i$ represent the sensitivity of bus i to line m, from bus p to bus q. These terms can be replaced by $F_q(m, i)$ and $K_q(m, i)$, termed the reactive power JBDF. Accordingly, (18) can be rewritten as

$$\Delta Q_m = \sum_{i=1}^{\mathrm{NB}} F_q(m, i)\Delta P_i + \sum_{i=1}^{\mathrm{NB}} K_q(m, i)\Delta Q_i \tag{19}$$

substituting (19) for ΔQ_m in (17)

$$Q_m = Q_m^0 + \sum_{i=1}^{\mathrm{NB}} F_q(m, i)\Delta P_i + \sum_{i=1}^{\mathrm{NB}} K_q(m, i)\Delta Q_i \tag{20}$$

Therefore the reactive power JBDF terms can be derived as follows

$$F_q(m, i) = \sum_{j=1}^{\mathrm{NB}} \frac{\partial |V_j|}{\partial P_i}\frac{\partial Q_m}{\partial |V_j|} + \sum_{j=1}^{\mathrm{NB}} \frac{\partial \delta_j}{\partial P_i}\frac{\partial Q_m}{\partial \delta_j}, \quad m = 1, 2, \ldots, \mathrm{NL} \tag{21}$$

and

$$K_q(m, i) = \sum_{j=1}^{\mathrm{NB}} \frac{\partial |V_j|}{\partial Q_i}\frac{\partial Q_m}{\partial |V_j|\lim\limits_{x\to\infty}} + \sum_{j=1}^{\mathrm{NB}} \frac{\partial \delta_j}{\partial Q_i}\frac{\partial Q_m}{\partial \delta_j}, \quad m = 1, 2, \ldots, \mathrm{NL} \tag{22}$$

In (21) and (22), the partial differential terms $\partial|V_j|/\partial P_i$, $\partial|V_j|/\partial Q_i$ and $\partial\delta_j|/\partial Q_i$ can be calculated in the Jacobian matrix of the base case power flow solution. As mentioned in the previous subsection, the summation of the differential terms in (21) and (22) can be curtailed to

$$F_q(m, i) = \left(\frac{\partial |V_p|}{\partial P_i}\right)\frac{\partial Q_m}{\partial |V_p|} + \left(\frac{\partial |V_q|}{\partial P_i}\right)\frac{\partial Q_m}{\partial |V_q|} + \left(\frac{\partial \delta_p}{\partial P_i}\right)\frac{\partial Q_m}{\partial \delta_p} + \left(\frac{\partial \delta_q}{\partial P_i}\right)\frac{\partial Q_m}{\partial \delta_q} \tag{23}$$

$$K_q(m, i) = \left(\frac{\partial |V_p|}{\partial Q_i}\right)\frac{\partial Q_m}{\partial |V_p|} + \left(\frac{\partial |V_q|}{\partial Q_i}\right)\frac{\partial Q_m}{\partial |V_q|} + \left(\frac{\partial \delta_p}{\partial Q_i}\right)\frac{\partial Q_m}{\partial \delta_p} + \left(\frac{\partial \delta_q}{\partial Q_i}\right)\frac{\partial Q_m}{\partial \delta_q} \tag{24}$$

Similarly, in (23) and (24), the partial differential terms also can be classified into two groups. One is the relationships between bus voltage and bus power injection; the other is the relationships between reactive-power line flow and bus voltage, by differentiating (2), the partial differential terms of $\partial Q_m/\partial|V_p|$, $\partial Q_m|/\partial|V_q|$, $\partial Q_m|/\partial\delta_p$ and $\partial Q_m/\partial\delta_q$ can be expressed as (25)–(28)

$$\frac{\partial Q_m}{\partial |V_p|} = -2|V_p^0|B_m + |V_q^0|B_m\cos(\delta_p^0 - \delta_q^0) - |V_q^0|G_m\sin(\delta_p^0 - \delta_q^0) \tag{25}$$

$$\frac{\partial Q_m}{\partial |V_q|} = |V_p^0|B_m\cos(\delta_p^0 - \delta_q^0) - |V_p^0|G_m\sin(\delta_p^0 - \delta_q^0) \tag{26}$$

$$\frac{\partial Q_m}{\partial \delta_p} = -|V_p^0||V_q^0|B_m\sin(\delta_p^0 - \delta_q^0) - |V_p^0||V_q^0|G_m\cos(\delta_p^0 - \delta_q^0) \tag{27}$$

and

$$\frac{\partial Q_m}{\partial \delta_q} = |V_p^0||V_q^0|B_m\sin(\delta_p^0 - \delta_q^0) + |V_p^0||V_q^0|G_m\cos(\delta_p^0 - \delta_q^0) \tag{28}$$

Similar to active power JBDF, using the above equations, the reactive power JBDF sensitivity factors can be calculated in base case loading conditions, and kept constant during real-time computation.

3 Solution procedure

For the application of economic dispatch and optimal power flow, line flow should be recomputed in each iteration, because of shifts in bus generation. In such applications, total system demands are assumed to remain unchanged during the iterations. If loading levels change from the base point, a new line flow base should be established. In conventional approaches, GSDF is only capable of handling shifts in generation, with total system load demands remaining unchanged. In contrast, GGDF can solve the conforming load change problem. Besides, ZBD and PTDF reflect only changes in bus active power injection. Our proposed JBDF method is capable of handling changes in conforming and non-conforming system demand across all buses as well as providing a precise reflection of the active and reactive power injection into the active power flow.

As shown in Fig. 2, the line flow base should be renewed when system demand changes from base case 1 to a new

doi: 10.1049/iet-gtd.2011.0429

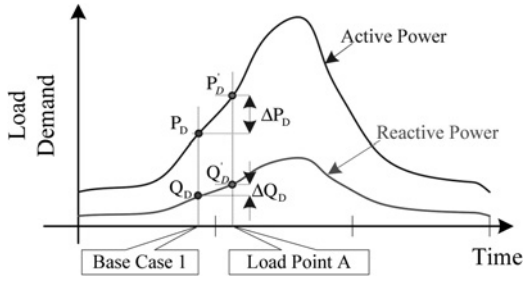

Fig. 2 *System demand curve*

point A. At this new loading point A, the amount of change in the active and reactive power demands of the bus can be expressed as increments from the base load. These incremental terms must be balanced by total active and reactive power generation. Before scheduling the generation of power by economic dispatch or optimal power flow, it can be assumed that increments in system demand should be absorbed by the reference bus generator. Consequently, changes in active and reactive power injection in each bus can be represented as (29) and (30), respectively. In load buses, the ΔP_i is equal to '$-\Delta P_{\mathrm{D}_i}$', and ΔQ_i equals '$-\Delta Q_{\mathrm{D}_i}$'.

$$\Delta P_i = \Delta P_{\mathrm{G}_i} - \Delta P_{\mathrm{D}_i} \tag{29}$$

$$\Delta Q_i = \Delta Q_{\mathrm{G}_i} - \Delta Q_{\mathrm{D}_i} \tag{30}$$

Therefore the increment power balance equations can be expressed as

$$\Delta P_{GR} = \sum_{i=1}^{\mathrm{NB}} \Delta P_{\mathrm{D}i} + \Delta P_{\mathrm{L}} \tag{31}$$

and

$$\Delta Q_{GR} = \sum_{i=1}^{\mathrm{NB}} \Delta Q_{\mathrm{D}i} + \Delta Q_{\mathrm{L}} \tag{32}$$

where ΔP_{GR} and ΔQ_{GR} denote increments in active and reactive power in reference bus R; ΔP_{Di} and ΔQ_{Di} represent increments in active and reactive power demand in bus i. In addition, ΔP_{L} and ΔQ_{D} are the increments in active and reactive power loss. There is no doubt that any changes in bus injection will result in differences in line flow and loss; therefore the active and reactive power loss models can be formulated by line flow as

$$P_{\mathrm{L}} = \sum_{m=1}^{\mathrm{NL}} (P_m^2 + Q_m^2) R_m \tag{33}$$

and

$$Q_{\mathrm{L}} = \sum_{m=1}^{\mathrm{NL}} (P_m^2 + Q_m^2) X_m \tag{34}$$

where R_m and X_m are the primitive resistance and reactance of line m; P_m and Q_m denote the active and reactive power line flow of line m. As bus voltage is assumed to be only unity in the above two equations, they represent nearly exact models of power losses. The incremental models of power loss can be expressed as

$$\Delta P_{\mathrm{L}} = \sum_{m=1}^{\mathrm{NL}} \frac{\partial P_{\mathrm{L}}}{\partial P_m} \Delta P_m + \sum_{m=1}^{\mathrm{NL}} \frac{\partial P_{\mathrm{L}}}{\partial Q_m} \Delta Q_m \tag{35}$$

$$\Delta Q_{\mathrm{L}} = \sum_{m=1}^{\mathrm{NL}} \frac{\partial Q_{\mathrm{L}}}{\partial P_m} \Delta P_m + \sum_{m=1}^{\mathrm{NL}} \frac{\partial Q_{\mathrm{L}}}{\partial Q_m} \Delta Q_m \tag{36}$$

By differentiating (33) and (34), the partial differential terms of $\partial P_{\mathrm{L}}/\partial P_m$, $\partial P_{\mathrm{L}}/\partial Q_m$, $\partial Q_{\mathrm{L}}/\partial P_m$ and $\partial Q_{\mathrm{L}}/\partial Q_m$ can be expressed as (35)–(38)

$$\frac{\partial P_{\mathrm{L}}}{\partial P_m} = 2R_m P_m \tag{37}$$

$$\frac{\partial P_{\mathrm{L}}}{\partial Q_m} = 2R_m Q_m \tag{38}$$

$$\frac{\partial Q_{\mathrm{L}}}{\partial P_m} = 2X_m P_m \tag{39}$$

$$\frac{\partial Q_{\mathrm{L}}}{\partial Q_m} = 2X_m Q_m \tag{40}$$

Substituting (5), (19) and (37)–(40) into (35) and (36), the incremental models of active and reactive power loss can be formulated as

$$\Delta P_{\mathrm{L}} = \sum_{m=1}^{\mathrm{NL}} 2R_m [F_p(m, i) P_m^0 + F_q(m, i) Q_m^0] \Delta P_i + \sum_{m=1}^{\mathrm{NL}} 2R_m [K_p(m, i) P_m^0 + K_q(m, i) Q_m^0] \Delta Q_i \tag{41}$$

$$\Delta Q_{\mathrm{L}} = \sum_{m=1}^{\mathrm{NL}} 2X_m [F_p(m, i) P_m^0 + F_q(m, i) Q_m^0] \Delta P_i + \sum_{m=1}^{\mathrm{NL}} 2X_m [K_p(m, i) P_m^0 + K_q(m, i) Q_m^0] \Delta Q_i \tag{42}$$

In (41) and (42), ΔP_i and ΔQ_i can be replaced by (29) and (30), respectively. By substituting (41) and (42) into (31) and (32), the power increments in the reference bus can be computed. Finally, the total power generation in the reference bus can be determined by adding base case power generation and incremental quantities resulting from incremental power loss.

In this paper, the problem of real-time active and reactive power flows calculation are both proposed and discussed. Since the JBDF algorithms for real-time active and reactive power flows calculation can be computed decoupled, the proposed JBDF method can be organised by the following steps:

Step 1: data input: system topology, bus data, line data, and base data
Step 2: solve for the base case line flows, P_m^0 and Q_m^0, using the Newton–Raphson method
Step 3: set up active power sensitivity factors, $F_p(m, i)$ and $K_p(m, i)$, by (11) and (12)
Step 4: set up reactive power sensitivity factors, $F_q(m, i)$ and $K_q(m, i)$, by (23) and (24)
Step 5: compute changes in system demand by $\Delta P_{\mathrm{D}i} = P_{Di} - P_{\mathrm{D}i}^0$, and $\Delta Q_{\mathrm{D}i} = Q_{\mathrm{D}i} - Q_{\mathrm{D}i}^0$

Step 6: compute changes in active and reactive power injection in the bus, using (29) and (30)
Step 7: compute active and reactive power flows using (6) and (20)
Step 8: stop calculations and print out results.

4 Numerical results

The mathematical models of JBDF for the calculation of active and reactive power flow are derived in Sections 2 and 3. Based on the above formulations, the proposed approach was coded using Matlab and executed on a Windows XP-based Intel® Core™2 Quad CPU Q6600 @2.4 GHz personal computer. To demonstrate the performance, the model was tested on standard IEEE 14-Bus and 30-Bus test systems. Three scenarios are assumed in Table 1, with two changes in system demand, simulating conforming and non-conforming increases from the base load. Because the accuracy of the line flow solution of the ZBD is much higher than that of the GSDF and GGDF approaches, as demonstrated in [6], the active and reactive power flow solutions of the proposed JBDF method were only compared to the ZBD method and Newton–Raphson method. In this paper, numerical mismatches and percentage error were all compared using Newton–Raphson solutions.

4.1 IEEE 14-bus system

In this subsection, the numerical results of the three scenarios for the IEEE 14-Bus system are used to verify the accuracy of the proposed approach. The simulation results are discussed as follows.

Table 1 Description of the scenarios

Scenarios	Description
scenario 1	conforming system demand increased by 10%
scenario 2	conforming system demand increased by 20%
scenario 3	non-conforming system demand changes

The numerical results of scenario 1 are shown in Table 2. Fig. 3*a* shows that the maximum active power flow mismatch of the JBDF was 0.334 MW in Line No. 10, and the corresponding maximum percentage error was 0.683% as shown in Fig. 3*b*. In contrast, the maximum active power flow mismatch of the ZBD was 2.29 MW in Line No. 1 as shown in Fig. 3*a*, and the maximum percentage error was 4.053% in Line No. 18, as shown in Fig. 3*b*. Additionally, Fig. 4*a* illustrates that the maximum reactive power flow mismatch of the JBDF was 0.224 Mvar in Line No. 10, and the maximum percentage error was 28.023% in Line No. 4 as shown in Fig. 4*b*. By contrast, the maximum reactive power flow mismatch of the ZBD was 9.534 Mvar in Line No. 1, as shown in Fig. 4*a*, and the maximum percentage error was 270.525% in Line No. 4, as shown in Fig. 4*b*.

In scenario 2, the numerical results of active and reactive power flow when conforming system demand increased by 20% are shown in Table 3. Fig. 3*a* shows that the maximum active power flow mismatch of the JBDF was 0.697 MW in Line No. 10, and the corresponding maximum percentage error was 1.3%, as shown in Fig. 3*b*; however, the maximum active power flow mismatch of the ZBD was 4.91 MW in Line No. 1 and the maximum percentage error was 7.388% in Line No. 18, as shown in Fig. 3*b*. In addition, Fig. 4*a* illustrates that the maximum reactive power flow mismatch of the JBDF was 0.467 Mvar in Line No. 10, and the maximum percentage error was 69.126% in Line No. 4, as shown in Fig. 4*b*. Nevertheless, the maximum reactive power flow mismatch of the ZBD was 18.884 Mvar in Line No. 1, as shown in Fig. 4*a*; and the maximum error% was 298.682% in Line No. 4, as shown in Fig. 4*b*.

We listed the percentage of non-conforming changes in system demand for scenario 3 in Table 4 to reflect the characteristics of changes in system demand for practical systems, and the numerical results of power flow are shown in Table 5. The maximum active power flow mismatch of the JBDF was 0.306 MW in Line No. 10, as shown in

Table 2 Power flow simulation result of scenario 1 for IEEE 14-Bus system (MW + jMvar)

Line no. (from bus to bus)	Method		
	Newton–Raphson	JBDF	ZBD
1 (1–2)	177.260 − j22.073	177.090 − j22.161	174.970 − j12.539
2 (1–5)	84.266 + j6.237	84.230 + j6.124	83.513 + j8.209
3 (2–3)	80.806 + j5.264	80.765 + j5.211	80.108 + j7.757
4 (2–4)	61.602 − j0.222	61.579 − j0.285	61.475 + j0.379
5 (2–5)	45.474 + j2.416	45.456 + j2.360	45.411 + j2.607
6 (3–4)	− 25.635 + j6.898	−25.649 + j6.849	−25.840 + j4.022
7 (4–5)	−67.370 + j16.510	−67.384 + j16.481	−67.666 + j13.603
8 (4–7)	30.708 − j8.583	30.651 − j8.521	30.855 − j7.187
9 (4–9)	17.566 + j0.565	17.522 + j0.583	17.679 + j1.045
10 (5–6)	48.874 + j12.668	48.540 + j12.892	48.315 + j15.453
11 (6–11)	8.268 + j4.846	8.263 + j4.833	8.069 + j4.190
12 (6–12)	8.626 + j2.889	8.623 + j2.884	8.561 + j2.774
13 (6–13)	19.659 + j8.469	19.652 + j8.457	19.498 + j8.038
14 (7–8)	0.000 − j18.986	0.000 − j18.959	0.000 − j17.283
15 (7–9)	30.708 + j8.435	30.710 + j8.425	30.877 + j8.440
16 (9–10)	5.590 + j3.754	5.593 + j3.762	5.764 + j4.355
17 (9–14)	10.234 + j3.429	10.236 + j3.432	10.353 + j3.763
18 (10–11)	− 4.323 − j2.661	−4.320 − j2.653	−4.148 − j2.057
19 (12–13)	1.827 + j0.944	1.827 + j0.944	1.779 + j0.863
20 (13–14)	6.363 + j2.505	6.358 + j2.497	6.207 + j2.094

doi: 10.1049/iet-gtd.2011.0429

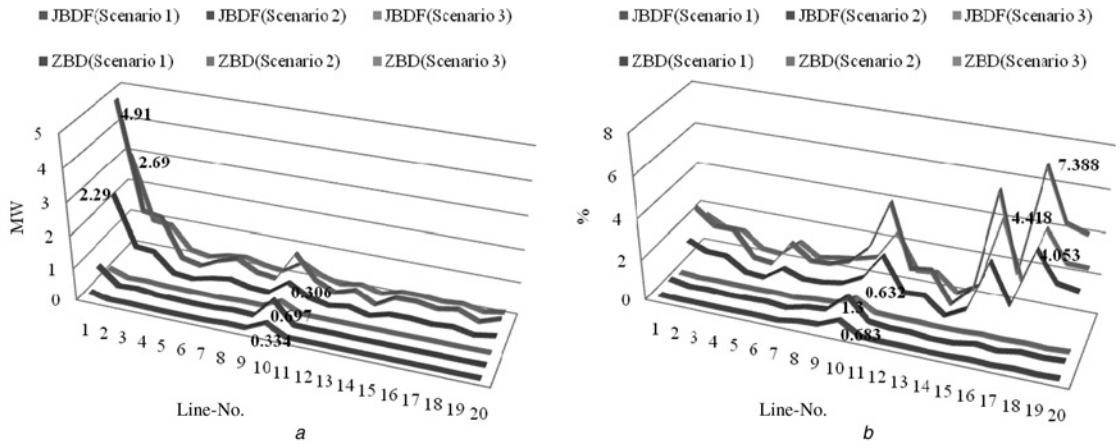

Fig. 3 *Mismatch and percentage error of active power flow compared with Newton–Raphson method for IEEE 14-Bus system*

a Mismatch
b Percentage error

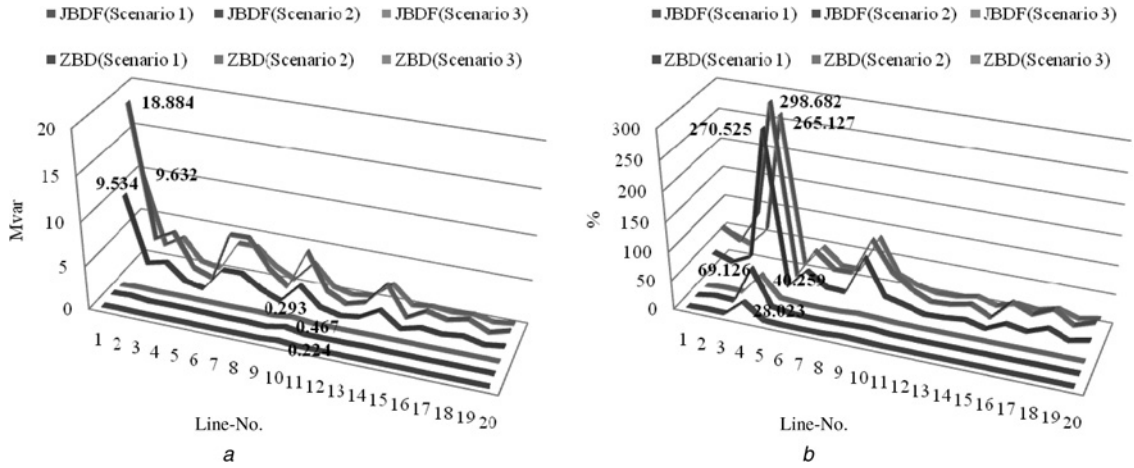

Fig. 4 *Mismatch and percentage error of reactive power flow compared with Newton–Raphson method for IEEE 14-Bus system*

a Mismatch
b Percentage error

Table 3 Power flow simulation result of scenario 2 for IEEE 14-Bus system (MW + jMvar)

Line no. (from bus to bus)	Method		
	Newton–Raphson	JBDF	ZBD
1 (1–2)	198.120 − j26.560	197.440 − j26.920	193.210 − j7.676
2 (1–5)	92.960 + j7.102	92.820 + j6.644	91.385 + j10.813
3 (2–3)	88.572 + j4.675	88.402 + j4.459	87.089 + j9.552
4 (2–4)	67.152 + j0.361	67.059 + j0.112	66.851 + j1.440
5 (2–5)	49.467 + j3.164	49.393 + j2.937	49.304 + j3.431
6 (3–4)	−27.853 + j9.756	−27.907 + j9.562	−28.291 + j3.907
7 (4–5)	− 73.492 + j18.335	−73.554 + j18.214	−74.117 + j12.457
8 (4–7)	33.385 − j8.448	33.275 − j8.320	33.684 − j5.652
9 (4–9)	19.074 + j0.975	18.994 + j1.003	19.306 + j1.926
10 (5–6)	53.608 + j11.811	52.911 + j12.278	52.461 + j17.399
11 (6–11)	9.154 + j5.867	9.132 + j5.813	8.744 + j4.527
12 (6–12)	9.458 + j3.245	9.446 + j3.228	9.323 + j3.007
13 (6–13)	21.556 + j9.595	21.530 + j9.545	21.221 + j8.708
14 (7–8)	0.000 − j20.743	0.000 − j20.636	0.000 − j17.283
15 (7–9)	33.385 + j9.985	33.394 + j9.948	33.728 + j9.977
16 (9–10)	5.985 + j3.558	5.997 + j3.592	6.339 + j4.778
17 (9–14)	11.075 + j3.427	11.085 + j3.438	11.319 + j4.099
18 (10–11)	−4.830 − j3.440	−4.813 − j3.405	−4.473 − j2.214
19 (12–13)	2.030 + j1.102	2.026 + j1.097	1.930 + j0.936
20 (13–14)	7.054 + j3.094	7.035 + j3.064	6.731 + j2.257

Table 4 Percentage of non-conforming system demand changes (scenario 3) in each bus for IEEE 14-Bus system

Bus no., %	1	2	3	4	5	6	7	8	9	10	11	12	13	14
ΔP_i	0	0	13	22	9	0	8	5	13	0	12	7	12	9
ΔQ_i	0	0	13	30	9	0	8	10	13	22	12	7	14	10

Fig. 3*a*, and the corresponding maximum percentage error was 0.32%, as shown in Fig. 3*b*. However, Fig. 3*a* shows that the maximum active power flow mismatch of the ZBD was 2.69 MW in Line No. 1, and Fig. 3*b* shows that the maximum percentage error was 4.148% in Line No. 16. Moreover, Fig. 4*a* shows that the maximum reactive power flow mismatch of the JBDF was 0.293 Mvar in Line No. 10, and the maximum percentage error was 40.259% in Line No. 4, as shown in Fig. 4*b*. In contrast, the maximum reactive power flow mismatch of the ZBD was 9.632 Mvar in Line No. 1, as shown in Fig. 4*a*, and the maximum percentage error was 265.127% in Line No. 4, as shown in Fig. 4*b*.

According to the numerical results mentioned above, the computation error of ZBD was greater than that using the JBDF, for all lines of the system. Furthermore, the total CPU time of JBDF was no more than 17 ms and far below the 91 ms used in the Newton–Raphson method. In addition, the accuracy of JBDF for active power flow calculation was better than that of JBDF for the calculation of reactive power flow. The outcomes indicate that the JBDF is superior to the ZBD. It appears that the proposed JBDF method is a fast and efficient estimation approach to line flow computation.

4.2 IEEE 30-Bus system

As in Subsection 4.1, we used the simulation results of the IEEE 30-Bus system to verify the accuracy of the proposed JBDF method.

The numerical results of conforming system demand with an increase of 10% for scenario 1 are shown in Table 6. Fig. 5*a* shows that the maximum active power flow mismatch of the JBDF was 0.316 MW in Line No. 15, and the maximum percentage error was 0.647% in Line No. 15, as shown in Fig. 5*b*; however, the maximum active power flow mismatch of the ZBD was 3.08 MW in Line No. 1, as shown in Fig. 5*a*, and the maximum percentage error was 8.923% in Line No. 33, as shown in Fig. 5*b*. Additionally, Fig. 6*a* shows that the maximum reactive power flow mismatch of the JBDF was 0.125 Mvar in Line No. 10, and the maximum percentage error was 2.328% in Line No. 6, as shown in Fig. 6*b*. Conversely, the maximum reactive power flow mismatch of the ZBD was 13.449 Mvar in Line No. 1, as shown in Fig. 6*a*, and the maximum percentage error was 184.809% in Line No. 41, as shown in Fig. 6*b*.

In scenario 2, the numerical results of active and reactive power flow are shown in Table 7. Fig. 5*a* indicates that the maximum active power flow mismatch of the JBDF was 0.646 MW in Line No. 15, and the maximum percentage error was 1.793% in Line No. 40, as shown in Fig. 5*b*. However, Fig. 5*a* shows that the maximum active power flow mismatch of the ZBD was 6.61 MW in Line No. 1, and the maximum percentage error was 16.59 % in Line No. 33, as shown in Fig. 5*b*. In addition, Fig. 6*a* illustrates that the maximum reactive power flow mismatch of the JBDF was 0.506 Mvar in Line No. 10, and the maximum percentage error was 9.577% in Line No. 5, as shown in Fig. 5*b*. On the other hand, the maximum reactive power flow mismatch of the ZBD was 26.691 Mvar in Line No. 1, as shown in Fig. 5*a*, and the maximum percentage error was 418.918% in Line No. 41, as shown in Fig. 5*b*.

In scenario 3, the percentage of changes in non-conforming system demand is listed in Table 8. The numerical results of complex power flow are shown in Table 9. As shown in the simulation results, the maximum active power flow

Table 5 Power flow simulation result of scenario 3 for IEEE 14-Bus system (MW + jMvar)

Line no. (from bus to bus)	Method		
	Newton–Raphson	JBDF	ZBD
1 (1–2)	181.280 − j22.958	181.010 − j23.079	178.320 − j13.326
2 (1–5)	86.348 + j6.344	86.289 + j6.172	85.370 + j8.173
3 (2–3)	83.348 + j5.058	83.277 + j4.963	82.415 + j8.170
4 (2–4)	63.746 − j0.256	63.706 − j0.360	63.503 + j0.423
5 (2–5)	46.724 + j2.412	46.694 + j2.325	46.589 + j2.647
6 (3–4)	−26.098 + j7.557	−26.119 + j7.485	−26.386 + j3.858
7 (4–5)	−70.956 + j17.211	−70.977 + j17.155	−71.307 + j13.533
8 (4–7)	30.309 − j8.518	30.261 − j8.431	30.511 − j6.730
9 (4–9)	17.332 + j0.707	17.296 + j0.734	17.473 + j1.306
10 (5–6)	48.396 + j12.373	48.090 + j12.666	47.871 + j15.405
11 (6–11)	8.603 + j5.177	8.596 + j5.157	8.386 + j4.591
12 (6–12)	8.626 + j2.896	8.622 + j2.890	8.559 + j2.790
13 (6–13)	19.967 + j8.730	19.958 + j8.714	19.791 + j8.324
14 (7–8)	0.000 − j19.527	0.000 − j19.492	0.000 − j17.283
15 (7–9)	30.309 + j9.088	30.312 + j9.079	30.491 + j8.892
16 (9–10)	4.433 + j4.171	4.437 + j4.181	4.617 + j4.686
17 (9–14)	9.872 + j3.358	9.876 + j3.363	10.001 + j3.645
18 (10–11)	−4.577 − j2.933	−4.574 − j2.923	−4.395 − j2.423
19 (12–13)	2.010 + j0.999	2.009 + j0.999	1.959 + j0.928
20 (13–14)	6.572 + j2.568	6.566 + j2.558	6.410 + j2.212

doi: 10.1049/iet-gtd.2011.0429

Table 6 Power flow simulation result of scenario 1 for IEEE 30-Bus system (MW + jMvar)

Line no. (from bus to bus)	Method		
	Newton–Raphson	JBDF	ZBD
1 (1–2)	195.830 − j23.243	195.610 − j23.343	192.750 − j9.794
2 (1–3)	97.763 + j7.415	97.706 + j7.278	96.682 + j11.333
3 (2–4)	47.848 + j6.703	47.824 + j6.642	47.659 + j7.860
4 (3–4)	91.256 − j5.490	91.244 − j5.460	90.965 + j1.208
5 (2–5)	91.069 + j3.404	91.018 + j3.335	90.132 + j6.732
6 (2–6)	66.400 + j2.534	66.361 + j2.477	66.067 + j5.194
7 (4–6)	79.618 − j19.660	79.613 − j19.601	79.558 − j12.188
8 (5–7)	−16.154 + j15.388	−16.170 + j15.352	−16.425 + j13.646
9 (6–7)	41.923 − j3.275	41.929 − j3.266	42.047 − j1.932
10 (6–8)	32.611 − j14.221	32.602 − j14.096	32.526 − j5.443
11 (6–9)	30.398 − j7.021	30.331 − j7.006	30.250 − j6.411
12 (6–10)	17.341 + j1.245	17.292 + j1.232	17.301 + j1.274
13 (9–11)	0.000 − j17.868	0.000 − j17.839	0.000 − j16.202
14 (9–10)	30.398 + j8.941	30.392 + j8.914	30.360 + j8.211
15 (4–12)	48.838 + j15.085	48.522 + j15.187	48.189 + j16.422
16 (12–13)	0.000 − j13.676	0.000 − j13.624	0.000 − j10.943
17 (12–14)	8.694 + j2.758	8.692 + j2.755	8.645 + j2.710
18 (12–15)	19.786 + j7.921	19.782 + j7.911	19.640 + j7.764
19 (12–16)	8.038 + j4.120	8.037 + j4.117	7.951 + j4.070
20 (14–15)	1.781 + j0.806	1.780 + j0.805	1.749 + j0.794
21 (16–17)	4.119 + j1.994	4.119 + j1.992	4.045 + j1.972
22 (15–18)	6.687 + j1.981	6.686 + j1.979	6.642 + j1.964
23 (18–19)	3.117 + j0.891	3.118 + j0.890	3.082 + j0.893
24 (19–20)	−7.339 − j2.862	−7.339 − j2.863	−7.373 − j2.857
25 (10–20)	9.878 + j3.892	9.876 + j3.890	9.890 + j3.840
26 (10–17)	5.808 + j4.465	5.807 + j4.467	5.876 + j4.473
27 (10–21)	17.323 + j11.012	17.319 + j11.007	17.260 + j10.905
28 (10–22)	8.351 + j5.055	8.349 + j5.052	8.313 + j4.995
29 (21–22)	−2.063 − j1.602	−2.065 − j1.604	−2.101 − j1.654
30 (15–23)	5.582 + j3.455	5.580 + j3.452	5.501 + j3.406
31 (22–24)	6.222 + j3.319	6.219 + j3.316	6.159 + j3.231
32 (23–24)	2.021 + j1.613	2.020 + j1.611	1.949 + j1.579
33 (24–25)	−1.390 + j1.759	−1.393 + j1.756	−1.514 + j1.658
34 (25–26)	3.905 + j2.613	3.904 + j2.611	3.895 + j2.597
35 (25–27)	−5.304 − j0.869	−5.307 − j0.872	−5.418 − j0.955
36 (28–27)	19.984 + j6.281	19.921 + j6.260	19.948 + j5.898
37 (27–29)	6.826 + j1.868	6.824 + j1.864	6.797 + j1.812
38 (27–30)	7.823 + j1.869	7.820 + j1.864	7.786 + j1.801
39 (29–30)	4.079 + j0.677	4.078 + j0.675	4.070 + j0.659
40 (8–28)	−0.539 + j3.149	−0.541 + j3.119	−0.561 + j1.636
41 (6–28)	20.600 + j0.590	20.598 + j0.587	20.684 + j1.680

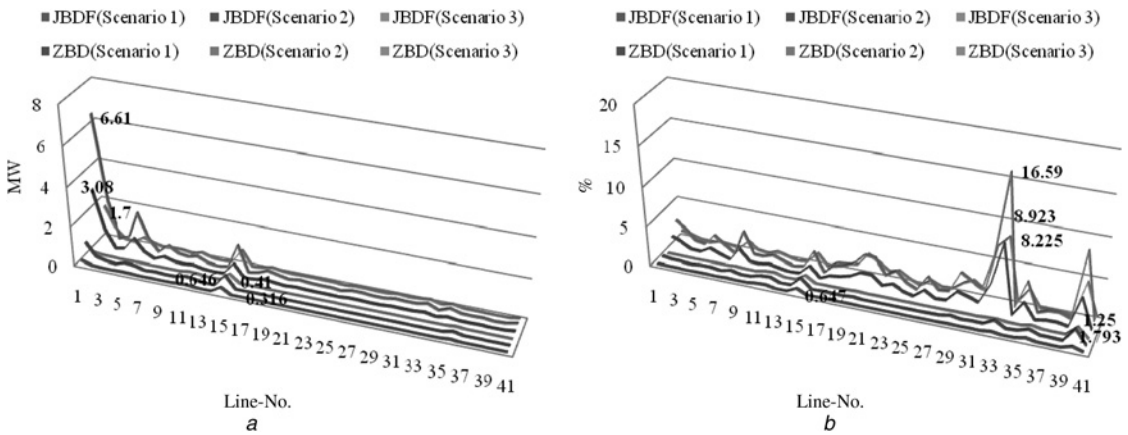

Fig. 5 *Mismatch and percentage error of active power flow compared with Newton–Raphson method for IEEE 30-Bus system*

a Mismatch
b Percentage error

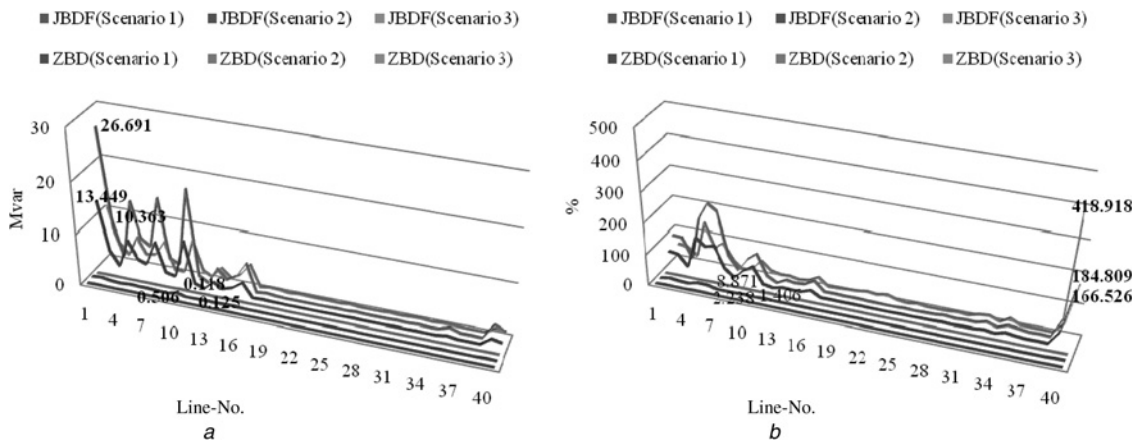

Fig. 6 *Mismatch and percentage error of reactive power flow compared with Newton–Raphson method for IEEE 30-Bus system*

a Mismatch
b Percentage error

Table 7 Power flow simulation result of scenario 2 for IEEE 30-Bus system (MW + jMvar)

Line no. (from bus to bus)	Method		
	Newton–Raphson	JBDF	ZBD
1 (1–2)	218.880 − j28.149	217.990 − j28.557	212.270 − j1.458
2 (1–3)	107.910 + j8.153	107.680 + j7.597	105.640 + j15.707
3 (2–4)	52.118 + j7.520	52.019 + j7.273	51.689 + j9.708
4 (3–4)	100.320 − j7.973	100.280 − j7.854	99.718 + j5.481
5 (2–5)	99.851 + j2.926	99.641 + j2.646	97.869 + j 9.439
6 (2–6)	72.551 + j2.590	72.394 + j2.361	71.806 + j7.793
7 (4–6)	87.168 − j23.582	87.148 − j23.344	87.039 − j8.518
8 (5–7)	−17.519 + j18.010	−17.581 + j17.869	−18.092 + j14.456
9 (6–7)	45.721 − j4.363	45.745 − j4.325	45.981 − j1.657
10 (6–8)	35.660 − j20.517	35.625 − j20.011	35.474 − j2.706
11 (6–9)	33.158 − j6.230	33.012 − j6.227	32.849 − j5.038
12 (6–10)	18.892 + j2.036	18.791 + j1.982	18.810 + j2.065
13 (9–11)	0.000 − j19.595	0.000 − j19.475	0.000 − j16.202
14 (9–10)	33.158 + j11.126	33.133 + j11.019	33.070 + j9.612
15 (4–12)	53.400 + j15.794	52.754 + j15.957	52.088 + j18.426
16 (12–13)	0.000 − j16.515	0.000 − j16.305	0.000 − j10.943
17 (12–14)	9.510 + j3.061	9.503 + j3.048	9.409+ j2.958
18 (12–15)	21.645 + j8.819	21.628 + j8.780	21.344 + j8.485
19 (12–16)	8.804 + j4.607	8.801 + j4.592	8.629 + j4.498
20 (14–15)	1.959 + j0.909	1.956 + j0.905	1.894 + j0.881
21 (16–17)	4.519 + j2.269	4.520 + j2.261	4.373 + j2.220
22 (15–18)	7.321 + j2.215	7.319 + j2.208	7.230 + j2.178
23 (18–19)	3.421 + j1.013	3.422 + j1.011	3.351 + j1.016
24 (19–20)	−7.987 − j3.083	−7.986 − j3.085	−8.055 − j3.074
25 (10–20)	10.769 + j4.235	10.763 + j4.226	10.792 + j4.127
26 (10–17)	6.313 + j4.787	6.311 + j4.793	6.449 + j4.805
27 (10–21)	18.900 + j12.084	18.886 + j12.064	18.767 + j11.859
28 (10–22)	9.109 + j5.554	9.101 + j5.543	9.030 + j5.429
29 (21–22)	−2.265 − j1.711	−2.272 − j1.718	−2.344 − j1.820
30 (15–23)	6.105 + j3.857	6.099 + j3.845	5.941 + j3.753
31 (22–24)	6.766 + j3.682	6.753 + j3.669	6.632 + j3.500
32 (23–24)	2.215 + j1.837	2.211 + j1.829	2.068 + j1.766
33 (24–25)	−1.536 + j1.654	−1.549 + j1.639	−1.791 + j1.444
34 (25–26)	4.267 + j2.860	4.263 + j2.855	4.245 + j2.827
35 (25–27)	−5.813 − j1.223	−5.823 − j1.233	−6.045 − j1.399
36 (28–27)	21.875 + j7.429	21.745 + j7.332	21.799 + j6.608
37 (27–29)	7.465 + j2.075	7.457 + j2.059	7.404 + j1.955
38 (27–30)	8.558 + j2.084	8.548 + j2.065	8.479 + j1.938
39 (29–30)	4.456 + j0.750	4.453 + j0.745	4.437 + j0.712
40 (8–28)	−0.541 + j4.452	−0.551 + j4.331	−0.590 + j1.365
41 (6–28)	22.513 + j0.519	22.506 + j0.506	22.678 + j2.692

doi: 10.1049/iet-gtd.2011.0429

mismatch of the JBDF was 0.41 MW in Line No. 15, as shown in Fig. 5*a*, and the maximum percentage error was 1.25 % in Line No. 40, as shown in Fig. 5*b*. However, Fig. 5*a* shows that the maximum active power flow mismatch of the ZBD was 1.7 MW in Line No. 1, and Fig. 5*b* shows that the maximum error was 8.225% in Line

Table 8 Percentage of non-conforming system demand changes (scenario 3) in each bus for IEEE 30-Bus system

Bus no., %	1	2	3	4	5	6	7	8	9	10
ΔP_i	0	0	15	25	0	18	6	0	5	24
ΔQ_i	0	0	10	30	0	8	25	0	20	14
Bus no., %	11	12	13	14	15	16	17	18	19	20
ΔP_i	0	28	0	0	5	30	15	6	30	11
ΔQ	0	18	0	6	27	30	12	5	7	6
Bus no., %	21	22	23	24	25	26	27	28	29	30
ΔP_i	7	15	12	0	16	11	30	14	25	0
ΔQ	23	6	25	16	6	22	28	24	5	10

Table 9 Power flow simulation result of scenario 3 for IEEE 30-Bus system (MW + jMvar)

Line no. (from bus-to bus)	Method		
	Newton–Raphson	JBDF	ZBD
1 (1–2)	185.520 − j20.947	185.420 − j20.968	183.820 − j10.584
2 (1–3)	94.759 + j8.078	94.729 + j7.993	94.112 + j11.592
3 (2–4)	47.779 + j7.131	47.758 + j7.075	47.639 + j8.549
4 (3–4)	88.360 − j3.994	88.353 − j3.994	88.280 + j1.476
5 (2–5)	85.025+ j3.821	85.005 + j3.816	84.624 + j6.031
6 (2–6)	65.061 + j3.158	65.033 + j3.114	64.846 + j5.727
7 (4–6)	74.311 − j18.586	74.314 − j18.533	74.407 − j13.010
8 (5–7)	−12.318 + j14.642	−12.334 + j14.612	−12.473 + j14.875
9 (6–7)	37.012 − j1.359	37.023 − j1.340	37.165 − j1.535
10 (6–8)	29.965 − j14.915	29.957 − j14.797	29.897 − j7.988
11 (6–9)	31.498 − j6.424	31.404 − j6.434	31.277 − j5.231
12 (6–10)	17.958 + j1.750	17.890 + j1.710	17.899 + j1.959
13 (9–11)	0.000 − j18.676	0.000 − j18.634	0.000 − j16.202
14 (9–10)	31.498 + j10.226	31.488 + j10.177	31.440 + j9.442
15 (4–12)	50.108 + j15.804	49.698 + j15.864	49.332 + j17.683
16 (12–13)	0.000 − j15.237	0.000 − j15.171	0.000 − j10.943
17 (12–14)	8.286 + j2.861	8.283 + j2.857	8.221 + j2.760
18 (12–15)	19.282 + j8.649	19.273 + j8.633	19.109 + j8.237
19 (12–16)	8.205 + j4.638	8.201 + j4.630	8.115 + j4.315
20 (14–15)	2.000 + j0.987	1.998 + j0.984	1.946 + j0.907
21 (16–17)	3.578 + j2.139	3.577 + j2.134	3.509 + j1.858
22 (15–18)	7.352 + j2.012	7.348 + j2.003	7.279 + j1.826
23 (18–19)	3.901 + j0.946	3.900 + j0.943	3.848 + j0.799
24 (19–20)	−8.459 − j2.712	−8.459 − j2.714	−8.508 − j2.849
25 (10–20)	11.046 + j3.772	11.041 + j3.762	11.047 + j3.804
26 (10–17)	6.800 + j4.441	6.801 + j4.445	6.863 + j4.703
27 (10–21)	16.508 + j12.137	16.505 + j12.134	16.448 + j12.049
28 (10–22)	7.910 + j5.566	7.908 + j5.564	7.875 + j5.520
29 (21–22)	−2.354 − j1.933	−2.355 − j1.933	−2.388 − j1.966
30 (15–23)	5.041 + j3.913	5.039 + j3.910	4.938 + j3.706
31 (22–24)	5.492 + j3.500	5.490 + j3.500	5.435 + j3.445
32 (23–24)	1.419 + j1.835	1.417 + j1.833	1.322 + j1.640
33 (24–25)	−1.843 + j1.776	−1.847 + j1.776	−1.995 + j1.530
34 (25–26)	3.945 + j2.896	3.943 + j2.893	3.930 + j2.873
35 (25–27)	−5.801 − j1.141	−5.802 − j1.137	−5.934 − j1.359
36 (28–27)	19.745 + j6.415	19.690 + j6.397	19.721 + j6.217
37 (27–29)	6.635 + j1.805	6.634 + j1.803	6.621 + j1.780
38 (27–30)	7.272 + j1.808	7.271 + j1.807	7.262 + j1.788
39 (29–30)	3.534 + j0.669	3.534 + j0.669	3.534 + j0.671
40 (8–28)	−0.167 + j3.277	−0.169 + j3.248	−0.175 + j2.119
41 (6–28)	19.985 + j0.584	19.985 + j0.580	20.094 + j1.557

No. 33. Additionally, Fig. 5*a* depicts the maximum reactive power flow mismatch of the JBDF is 0.118 Mvar in Line No. 10, and the maximum percentage error was 1.406% in Line No. 6 as shown in Fig. 5*b*. In contrast, the maximum reactive power flow mismatch of the ZBD was 10.363 Mvar in Line No. 1, as shown in Fig. 5*a*; and the maximum error was 166.25% in Line No. 41, as shown in Fig. 5*b*.

The simulation results of IEEE 30-Bus system are similar to those of the IEEE 14-Bus system. According to the numerical results, the accuracy of JBDF approach is higher than that of the ZBD approach, compared with the Newton–Raphson method. Moreover, the accuracy of JBDF for the calculation of active power flow is much higher than that of JBDF for the calculation of reactive power flow.

4.3 Discussion

Summing up the numerical results, we conclude that the overall performance of JBDF is superior to that of well-known sensitivity factors, such as GSDF, GGDF, ZBD and PTDF. Additionally, the accuracy of JBDF for active power calculation is better than that of reactive power flow calculation, because reactive power is more sensitive to voltage. In other words, reactive power is far more non-linear than active power; resulting in greater error in the calculation of reactive power flow. Although the percentage error of reactive power flow in some line segments was too large, this was caused by low reactive power flow and the errors were amplified because of small deviations between the simulation results of Newton–Raphson method and the JBDF approach, divided by the results of the Newton–Raphson method. For instance, in Section 4.1, the maximum percentage error of the JBDF for reactive power calculation of scenario 2 was 69.126% in Line No. 4 and its corresponding mismatch was only 0.24964 Mvar. However, the result of the Newton–Raphson method was 0.36114 Mvar, setting the calculated percentage error at 69.126%. In a per unit system, this accounts for just 0.0024964 pu on 100 MVA base value. Consequently, it is doubtless that the mismatches of these line segments are very small, and they would not affect the application of the proposed JBDF approach. In real-time applications, it is worth noting that greater error in line flow calculation occurs for large changes in system load demand. If the degree of error is unacceptable, the base case power flow must be executed again to ensure an acceptable solution. In this paper, we simulated changes of 20% in system demand from base case, and the degree of error was acceptable. The accuracy was the best among the well-known sensitivity factors.

5 Conclusions

In this paper, a new network sensitivity factor, JBDF, for real-time line flow calculation is proposed. It overcomes the active and reactive power flow problem without any iterations following changes in load demand and improves on the accuracy of the ZBD sensitivity factor, thereby eliminating the convergence problem during real-time applications. Using this new method, complex power flow can easily be calculated, reflecting changes in bus complex power injection into the line flows. As shown by the numerical results, the complex power flow calculated by the proposed approach are nearly the same as those using the exact method and the speed required to reach a solution was much faster. The proposed approach demonstrates a high degree of accuracy and rapid execution times in the computation of line flow. It is therefore well suited to real-time applications without the risk of divergence.

6 Acknowledgment

The authors would like to thank the National Science Council of Taiwan, R.O.C., for the financial support under Grant No. NSC-97-2221-E-270-014-MY3.

7 References

1 Wood, A.J., Wollenberg, B.F.: 'Power generation, operation and control' (Wiley, New York, 1984)
2 Stott, B., Alsac, O.: 'Fast decoupled load flow', *IEEE Trans. Power Appar. Syst.*, 1974, **PAS-93**, (3), pp. 859–869
3 Chen, Y., Shen, C.: 'A Jacobian-free Newton-GMRES(m) method with adaptive preconditioner and its application for power flow calculations', *IEEE Trans. Power Syst.*, 2006, **21**, (3), pp. 1096–1103
4 Marinho, J.M.T., Taranto, G.N.: 'A hybrid three-phase single-phase power flow formulation', *IEEE Trans. Power Syst.*, 2008, **23**, (3), pp. 1603–1670
5 Milano, F.: 'Continuous Newton's method for power flow analysis', *IEEE Trans. Power Syst.*, 2009, **24**, (1), pp. 50–57
6 Salgado, R.S., Zeitune, A.F.: 'Power flow solutions through tensor methods', *IET Gener. Transm. Distrib.*, 2009, **3**, (5), pp. 413–424
7 Lourenço, E.M., Costa, A.S., Ribeiro, R.P. Jr.: 'Steady-state solution for power networks modeled at bus section level', *IEEE Trans. Power Syst.*, 2010, **25**, (1), pp. 10–20
8 Zhang, Y.S., Chiang, H.D.: 'Fast Newton-FGMRES solver for large-scale power flow study', *IEEE Trans. Power Syst.*, 2010, **25**, (2), pp. 769–776
9 Ng, W.Y.: 'Generalized generation distribution factors for power system security evaluations', *IEEE Trans. Power Appar. Syst.*, 1981, **PAS-100**, pp. 1001–1005
10 Lin, C.E., Chen, S.T., Huang, C.L.: 'A two-step sensitivity approach for real-time line flow calculation', *Electric Power Syst. Res.*, 1991, **21**, (1), pp. 63–69
11 Chang, Y.C., Yang, W.T., Liu, C.C.: 'Improvements on the line outage distribution factor for power system security analysis', *Electric Power Syst. Res.*, 1993, **26**, pp. 231–236
12 Chang, Y.C., Yang, W.T., Liu, C.C.: 'A new method for calculating loss coefficients', *IEEE Trans. Power Syst.*, 1994, **9**, (3), pp. 1665–1671
13 Chang, Y.C., Liu, C.C., Yang, W.T.: 'Real-time line flow calculation using a new sensitivity method', *Electric Power Syst. Res.*, 1992, **24**, (2), pp. 127–133
14 Jan, R.M., Chen, N.: 'Applications of the fast Newton–Raphson economic dispatch and reactive power/voltage dispatch by sensitivity factors to optimal power flow', *IEEE Trans. Energy Convers.*, 1995, **10**, (2), pp. 293–301
15 Lin, C.E., Chen, S.T., Huang, C.L.: 'A direct Newton-Raphson economic dispatch', *IEEE Trans. Power Syst.*, 1992, **7**, (3), pp. 1149–1153
16 Fang, D.Z., Sun, W., Xue, Z.Y.: 'Optimal generation rescheduling with sensitivity-based transient stability constraints', *IET Gener. Transm. Distrib.*, 2010, **4**, (9), pp. 1044–1051
17 Ruiz, P.A., Sauer, P.W.: 'Voltage and reactive power estimation for contingency analysis using sensitivities', *IEEE Trans. Power Syst.*, 2007, **22**, (2), pp. 639–647
18 Parida, S.K., Singh, S.N., Srivastava, S.C.: 'Reactive power cost allocation by using a value-based approach', *IET Gener. Transm. Distrib.*, 2009, **3**, (9), pp. 872–884
19 Jupe, S.C.E., Taylor, P.C.: 'Distributed generation output control for network power flow management', *IET Renew. Power Gener.*, 2009, **3**, (4), pp. 371–386
20 Zhou, Q., Bialek, J.W.: 'Generation curtailment to manage voltage constraints in distribution networks', *IET Gener. Transm. Distrib.*, 2007, **1**, (3), pp. 492–498
21 Teng, J.H., Lu, C.N.: 'Optimum fault current limiter placement with search space reduction technique', *IET Gener. Transm. Distrib.*, 2010, **4**, (4), pp. 485–494
22 Ayres, H.M., Freitas, W., De Almeida, M.C., Da Silva, L.C.P.: 'Method for determining the maximum allowable penetration level of distributed generation without steady-state voltage violations', *IET Gener. Transm. Distrib.*, 2010, **4**, (4), pp. 495–508
23 Peschon, J., Piercy, D.S., Tinney, W.F., Tveit, O.J.: 'Sensitivity in power systems', *IEEE Trans. Power Appar. Syst.*, 1968, **PAS-87**, (8), pp. 1687–1696
24 Salgado, R., Simões Costa, A.J.A., Medeiros, A.D.R.: 'Overload corrective control through least squares techniques'. Proc. IEEE Athens Power Tech, Athens, Greece, September 1993

doi: 10.1049/iet-gtd.2011.0429